



## **RETROFIT OF SLAB-COLUMN CONNECTIONS USING CFRP**

**Gaur P JOHNSON<sup>1</sup> and Ian N ROBERTSON<sup>2</sup>**

### **SUMMARY**

Slab-column connections in flat slab buildings with inadequate design and detailing for seismic events have resulted in considerable structural damage and loss of life during past earthquakes. The large world wide inventory of substandard flat slab buildings requires simple, innovative, unobtrusive and economical techniques to mitigate the disastrous effects of future earthquakes. The use of carbon fiber reinforced polymer (CFRP) composite fabric bonded to the surface of concrete members is comparatively simple, quick and virtually unnoticeable after installation. Around the world, the use of composites has become routine for increasing both the flexural and shear strength of reinforced and prestressed concrete beams. Earthquake retrofit of bridge and building structures has relied heavily on composite wrapping of columns, beams and joints to provide confinement and increase ductility. This paper presents the results of cyclic testing of three large-scale reinforced concrete slab-column connections. Each of these specimens is a half-scale model of an interior slab-column connection common to flat-plate buildings. While supporting a slab gravity load, the specimens were subjected to a cyclic lateral loading protocol. The test specimens simulated older non-seismic flat-slab construction, which is in need of retrofit to resist anticipated future earthquakes. The designed connections had no slab shear reinforcement to prevent punching shear failure or continuity reinforcement to prevent progressive collapse. The control specimen failed in punching shear. Two nominally identical specimens were retrofitted with CFRP sheets applied to the top surface of the slab. The additional flexural strength and stiffness of the retrofit connections resulted in larger loads at the connection when subjected to lateral cycling, but did not prevent a punching shear failure. After these cyclic lateral tests were performed two additional slab-column connections were tested in direct punching to evaluate the possible use of CFRP studs as retrofit shear reinforcement. The first direct punching specimen was reinforced similar to the lateral test control specimen. The second was retrofitted using CFRP headed stud reinforcing. Although the punching strength only increased slightly, the CFRP headed studs provided significant additional ductility indicating good potential as a seismic retrofit.

### **INTRODUCTION**

In the 1950s, the trend towards lighter and more flexible construction configurations led to increased usage of flat plate construction—particularly for medium to high rise office and residential buildings [1]. Reinforced concrete flat plate construction has been and continues to be used as an economical structural

---

<sup>1</sup> Graduate Research Assistant, University of Hawaii at Manoa, Hawaii, USA

<sup>2</sup> Associate Professor, University of Hawaii at Manoa, Hawaii, USA

system for many buildings. In moderate and high seismic regions, flat plate structures are supplemented with either a moment frame or shear wall lateral resisting system. Today, ductile detailing for all structural connections, including for those which are “gravity load only,” is a key concept that was learned initially as a result of the failures observed during the 1971 San Fernando earthquake [1]. All the “gravity load only” slab column connections in a flat plate structure must maintain their capacity at the maximum displacement of the lateral system. During this lateral deformation the brittle failure mode of slab punching can occur. A punching shear failure, generated by the combination of the gravity loading and seismically induced unbalanced moment in the slab, can occur with little or no warning and has resulted in the progressive collapse of these types of structures. In the 1985 Mexico City earthquake, 91 flat plate buildings collapsed and 44 were severely damaged due to punching failure [2].

Structural engineers are often required to upgrade or retrofit existing buildings to meet current seismic design requirements or for new uses such as increased live load requirements. Seismic retrofit considerations are now commonplace. In the case of retrofit analysis of older buildings, it is often beneficial to include the additional lateral resistance provided by the slab-column frames as this may substantially reduce the cost of the overall building retrofit [3].

Prior to the ACI code revisions in the 1970s, which began to reflect ductile detailing lessons learned, reinforcing for flat slab systems did not require continuity of top and bottom reinforcement. Top reinforcing, used for negative bending, could be completely curtailed away from the column supports. Bottom reinforcing was only required to extend into supports by 150 mm (6 inches). It is now well known that positive bending can occur at the face of supports during lateral displacements inducing a bond failure at these short embedment locations. Due to the inadequacies of the pre-1971 design codes, there is a need to understand the behavior of the structures designed to these codes and to develop ways to upgrade these structures to provide an acceptable level of seismic safety.

The authors have begun to investigate different techniques to successfully retrofit flat-plate slab-column connections in a cost-effective way. Previous studies have been performed on repair techniques for damaged ductile slab-column connections using steel plates and through-bolting [4]. This technique could also be used to upgrade the performance of non-ductile pre-1971 connections, however, the aesthetic impact to the existing structure is a potential drawback. In a prior study the authors evaluated the repair of previously damaged ductile, slab-column connections using carbon fiber reinforced polymer (CFRP). One such repair was effective at restoring the peak lateral load resistance and initial stiffness of the undamaged connection [5]. These connections all contained internal slab shear reinforcement which was effective at preventing punching shear failure.

This paper reports the results of testing performed on large scale slab column connections, designed with pre-1971 non-ductile reinforcing and detailing, that were retrofitted with CFRP sheets epoxied to the slab surface. Three half-scale connections were subjected to a cyclic lateral loading routine while supporting a slab gravity load equivalent to dead load plus 30 percent of the design live load.

## **TESTING PROGRAM**

### **Lateral Loading Test Specimens**

Each specimen represents a half-scale model of an interior flat-plate slab column connection (Figure 1). The gravity load applied during the test is equivalent to a loading on the full-scale structure of the total dead load plus 30 percent of the floor live load. This gravity loading results in an effective shear stress at the critical perimeter equal to 25 percent of the direct punching shear capacity of the concrete—defined by the ACI 318 Building Code [6].

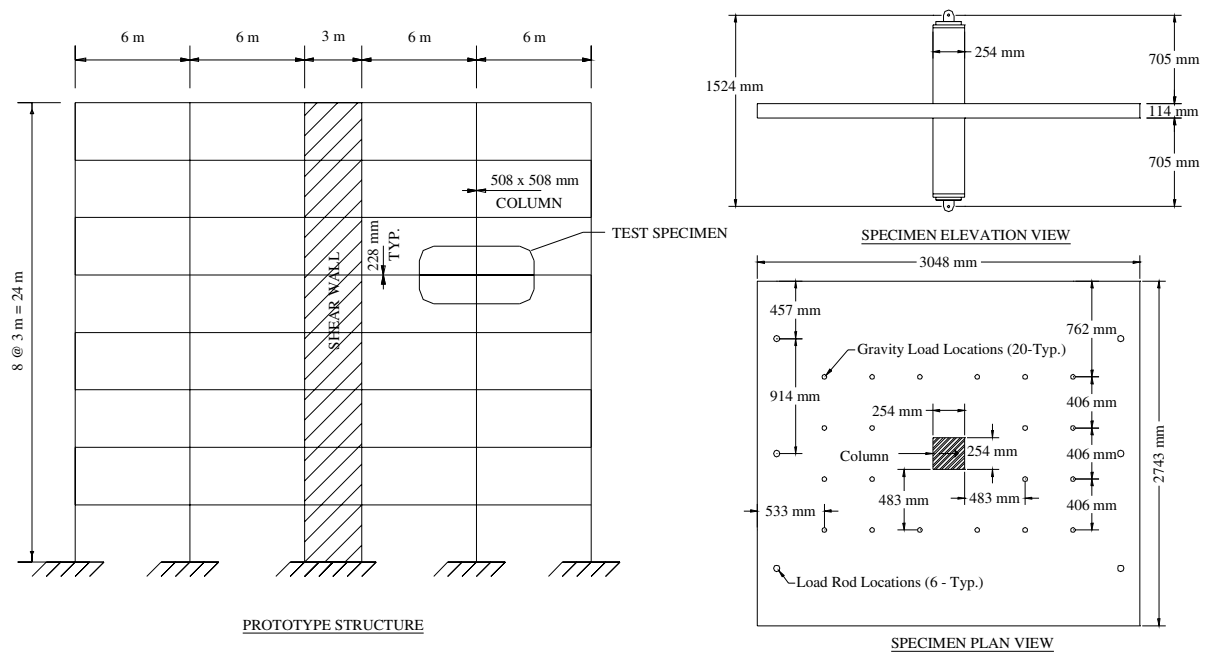


**Figure 1-Prototype Building and Test Specimen.**

The specimens were designed using the ACI 318-63 Building Code which does not require continuous bottom reinforcement through column lines. No shear reinforcing was included since the concrete shear capacity was adequate for the code defined ultimate conditions. Two additional bottom reinforcing bars were added in the direction perpendicular to the direction of lateral loading to prevent total collapse of the specimens within the test frame. These added bars did not affect the behavior of the connection before punching failure. Figure 2 shows the steel reinforcing layout for all three specimens.

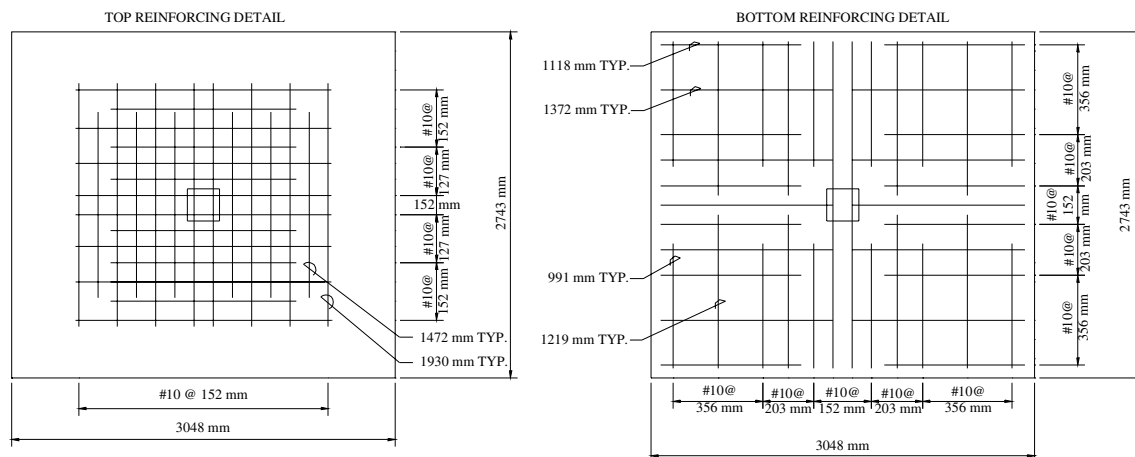
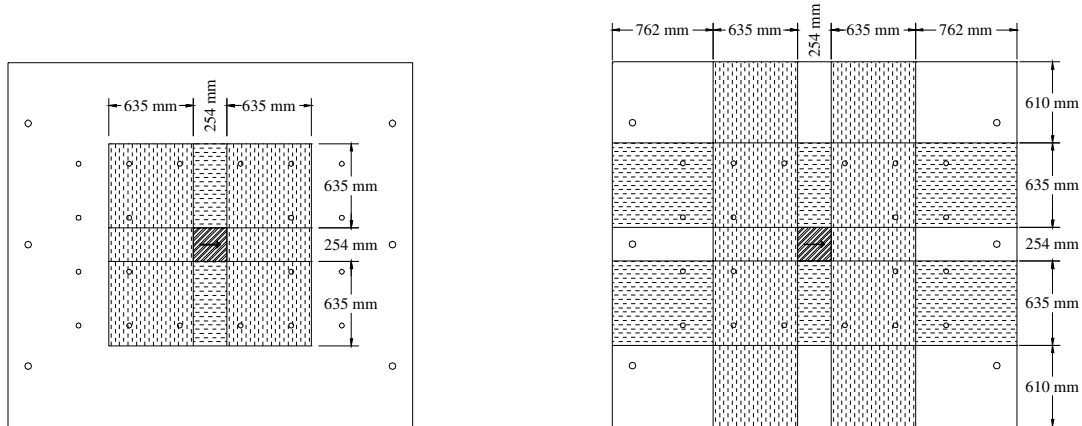
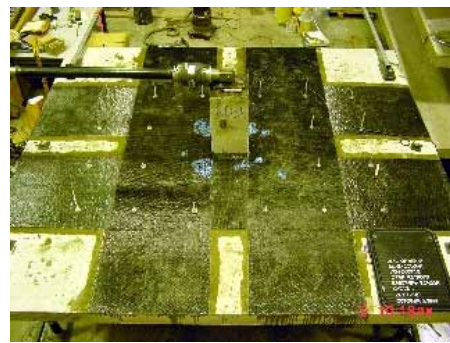


**Figure 2-Non-ductile Slab Reinforcing Details.**

Three specimens were tested: a control specimen, ND1C, with no retrofit; a second specimen, ND2R, with 635 mm wide CFRP unidirectional fabric applied to the top of the slab directly adjacent to the column and discontinued at 635 mm from the face of the 254 mm square column (Figure 3a); the third specimen, ND3R, was retrofitted the same as ND2R but with no curtailment of the CFRP fabric (Figure 3b). During the retrofitting, the concrete surface was prepared by roughening with a needle gun to remove the surface cement paste in the area of the application of CFRP, SikaWrap Hex 103C. The prepared surface was equivalent to a concrete surface profile (CSP) between 3 and 4 on the ICRI CSP scale [7]. SikaDur Hex 300 was used as the impregnating epoxy and bonding agent.



a) Specimen ND2R



b) Specimen ND3R

Figure 3-Top View of CFRP Retrofit of Non-Ductile Slab-Column Connections.

### Direct Punching Specimens

Two direct punching specimens were tested. These specimens were similar to the laterally loaded specimens. Both sets of specimens had 254 mm by 254 mm columns and were constructed with the same reinforcing ratio's within the column strip, middle strip and the  $c_2+3h$  equivalent beam width (described in the Analysis section of this paper). The direct punching slabs, however, had a thickness of 152 mm, with an average depth to tension reinforcing of 127 mm, and were 1524 mm by 1600 mm in plan dimension. The steel reinforcing layout

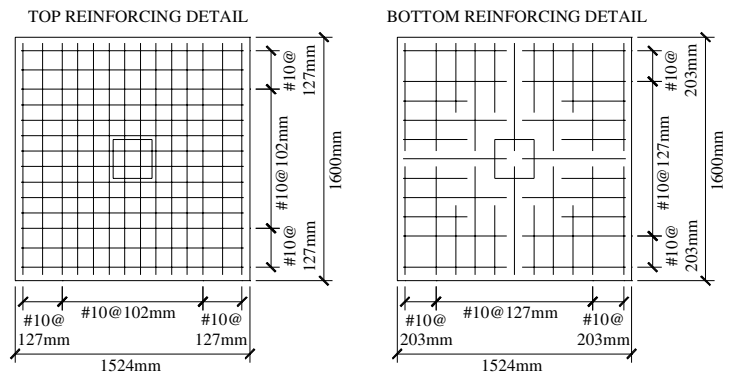


Figure 4-Specimen DPS1C & DPS2R slab reinforcing.

is shown in Figure 4.

Specimen DPS1C was the control specimen for the direct punching tests and contained only the reinforcing shown in Figure 4. Specimen DPS2R was retrofitted with 48-6.4mm diameter CFRP shear studs (Figure 5). These studs were installed in a configuration similar to shear stirrups—in eight rows of six studs. Each stud was installed as seen in Figure 4. Two rows of studs were placed starting at each column face at 140 mm apart (Figure 6). The stud spacing was 76 mm on center, with the first studs located 38 mm from the face of the column.

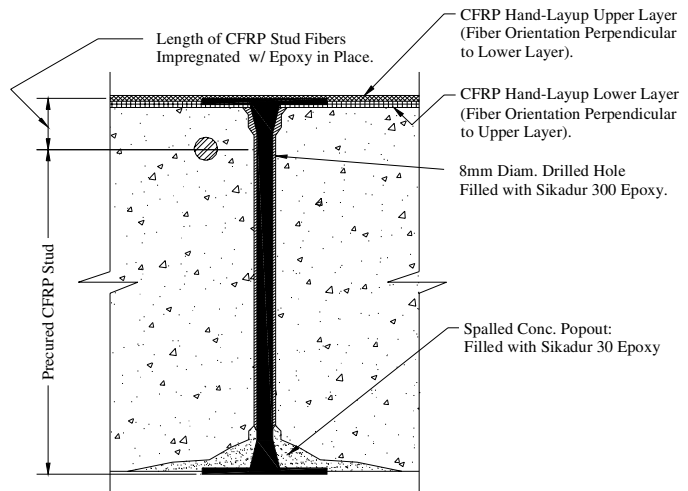


Figure 5-CFRP Stud Detail.



Figure 6-Specimen DPS2R: Top of Slab (left) and upside down in Direct Punching Test Frame (right).

**Test Displacement Routine**

For the cyclic test specimens, the loading routine was performed in two phases: Phase I consisted of both positive and negative cycling at each drift level up to 5 percent (limitation of the actuator); Phase II consisted of cycling up to 10 percent drift, but only in the positive drift direction (Figure 7). This protocol gradually increases the drift level from +/- 0.1% to +/- 5% in Phase I and from +7% to +10% in Phase II. To evaluate the loss of strength and stiffness after repeated loading of the structure, each drift level cycle was repeated three times.

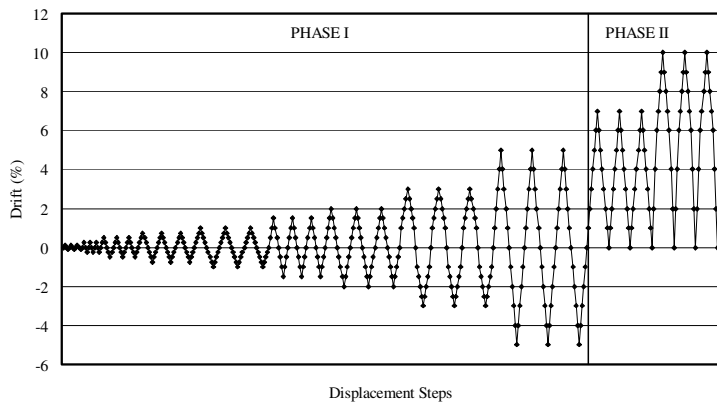
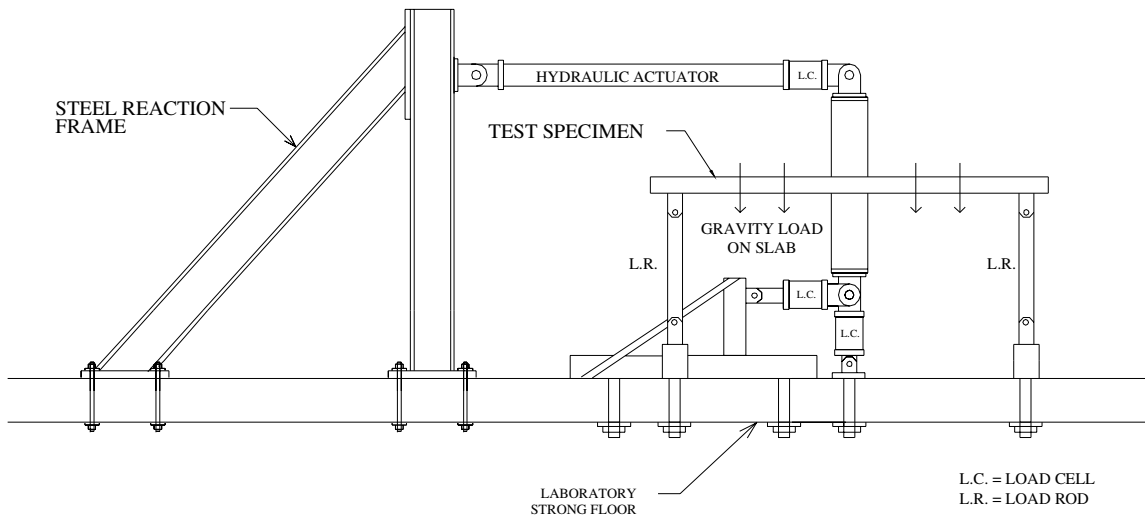


Figure 7-Lateral Displacement Routine.

## Test Setup and Instrumentation

The laterally loaded specimens were tested as shown in Figure 8. A pin support, with two load cells to monitor column axial load and shear, was located at mid-height of the column below the slab. Three pin ended vertical load rods at each edge of the slab prevented vertical displacement of the slab, but allowed free lateral movement and rotation, thus simulating mid-span conditions in the direction of loading. The cyclic lateral displacement routine (Figure 7) was applied to a pin connection at the mid-height of the column above the slab via an actuator with an internal linear varying displacement transducer (LVDT) and an inline load cell.



**Figure 8-Lateral Test Frame Configuration.**

## TEST RESULTS

### Material Properties

#### Concrete

The concrete used to make the specimens was supplied by a local ready-mix company with a specified compressive strength of 24 MPa. For each specimen, three 152 x 304 mm cylinders and two 152 x 152 x 533 mm beams were fabricated and cured in the same conditions as the slab. These were tested at the same age as the slab-column connections. The resulting concrete properties are listed in Table 1. The concrete compressive strength in Table 1 represents the actual strength of the concrete at the time of testing, and not the design 28 day strength.

**Table 1-Concrete Test Results**

Specimen	ND1C	ND2R	ND3R	DPS1C	DPS2R
Compressive Strength, $f_c$ (3 cylinders) (MPa)	29.6	27.7	24.4	59.8	53.4
Modulus of Elasticity, $E_c$ (1 Cylinder) (GPa)	17.4	15.8	22.1	30.3	33.4
Modulus of Rupture, $f_r$ (2 Beams) (MPa)	4.20	4.34	3.79	5.38	6.20
Poisson's Ratio, $\nu$ (1 Cylinder)	0.23	0.21	0.24	0.26	0.23

### Steel Reinforcing

The reinforcing used in both the slab and column in each specimen was specified as Grade 60 Type 2 deformed bars. The slab reinforcing was 10 mm diameter deformed bars with nominal yield strength of 420 MPa.

### Carbon Fiber Reinforced Polymer (CFRP) Properties

The cured and laminated CFRP has manufacturer reported structural properties as follows: Ultimate tensile strength of 958 MPa, a modulus of elasticity of 73.0 GPa, and an ultimate tensile strain of 1.33%. The cured laminate has a nominal thickness of 1.0 mm and a tensile strength of 9.74 kN / layer / cm. These properties were tested following ASTM D 3039/D 3039M – 95a Standard Test Method for Tensile Properties of Polymer Matrix Composite Materials to confirm the ultimate tensile strength. Steel plates were bonded to the ends of the 2.54 x 30 cm CFRP double layered coupon to facilitate end attachment to the tensile testing machine. The average ultimate tensile strength was determined to be 1017 MPa or a tensile strength of 8.80 kN / layer / cm. These properties are also assumed for the CFRP shear studs.

The bonding between substrate and CFRP was tested using a direct pull-off test. A minimum requirement of 1.38 kPa tensile strength or a concrete failure are commonly required to verify proper installation [8]. All pull-off tests failed in the concrete with average tensile bonding strength of 1.26 kPa and 1.23 kPa for the CFRP on specimens ND2R and ND3R respectively. The CFRP application was therefore bonded satisfactorily.

### Lateral Slab Cracking Behavior

During the lateral testing of a reinforced concrete slab-column connection, the slab cracking around the connection follows a typical pattern and cracking order. Figure 9 shows this typical crack progression under cyclic lateral loading to increasing drift levels. First, the gravity loads cause flexural cracks that propagate out from the column generally following the location of the top reinforcement (Figure 9a). Next, as lateral load is applied to the column, the existing flexural cracks widen and extend towards the slab edge. New flexural cracks form further from the column, and others form running diagonally from the column corners toward the corner of the specimen, opposite to the direction of the applied load (Figure 9b). At increased drift levels, torsional cracks begin to form adjacent to the column, running diagonally in the direction of the applied load (Figure 9c). Once the torsional and flexural crack patterns have fully developed, widening of the existing cracks continues with increasing drift levels until finally a punching failure occurs (Figure 9d).

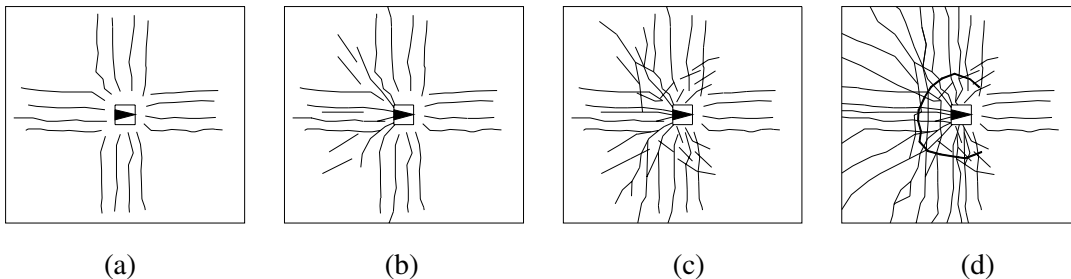


**Figure 9-Typical Crack Progression for a Cyclic Slab-Column Connection: (a) gravity load flexural cracking, (b) flexural cracking at low levels of drift, (c) torsional crack formation at increased levels of drift, (d) fully developed cracking with punch around column. Drift is in the direction of the arrow marked on the column.**

Generally, the retrofitted specimens cracked in a similar pattern to the control specimen. The application of CFRP to the slab restricted the view of crack formation around the column; however, the indication of

cracking was demonstrated through the de-bonding between the CFRP and the concrete as the test progressed.

#### *ND1C—Control Specimen*

This slab column connection experienced typical cracking as discussed previously and illustrated in Figure 8. The gravity load caused flexural cracking along the top reinforcement. The initiation of further flexural cracking occurred at 0.5% drift. Torsional cracking progressed in both positive and negative drift directions from about 1.5% drift to 5% drift. This specimen experienced extensive secondary flexural cracking and torsional cracking before punching failure occurred at a drift of 9%.

#### *ND2R—Curtailed CFRP Retrofit Specimen*

This slab experienced no initial cracking due to gravity loads. No cracking was noted until about 1.5% drift, where they were of the secondary flexural type, radiating away from the column in the areas without CFRP. Also, at 1.5% drift, de-bonding of the CFRP occurred in the areas that normally experience initial flexural cracking. At the 3% drift level, the CFRP experienced splitting transverse to the fiber orientation at about six inches from the column face in the area with only one layer applied perpendicular to the loading direction. The flexural cracking progressed until the slab failed in flexure at 3% drift. The failure location was just outside the curtailment of both the CFRP and top reinforcing steel, about 0.86 meters (34 inches) from the centerline of the column. This slab did not fail by a punching shear failure; instead it experienced a negative bending failure due to the lack of top reinforcement.

#### *ND3R—Continuous CFRP Retrofit Specimen*

This specimen behaved similar to ND2R with cracks not being visible until about the 2% drift level. These cracks were consistent with secondary flexural cracking as described for specimen ND2R. These cracks propagated radially away from the column in the areas without CFRP. When the cracks approached the CFRP they followed the edges of the fabric to the edge of the slab. De-bonding of the CFRP, initiating at 3.0% drift, was consistent with typical areas of initial cracking around the column and was in the location where the slab eventually punched. Also, later de-bonding was consistent with a prying type failure between the fabric and the slab surface—failing in the cement paste. This slab experienced splitting of the CFRP parallel to the direction of the fiber orientation in the immediate vicinity of the column where there was only one layer of CFRP placed transverse to the direction of loading. The splitting initiated at 5.0% drift. After the specimen was removed from the test frame, the de-bonded area of the CFRP removed to verify that the concrete slab had punched under the CFRP and the de-bonding was a result of prying of the punched section away from the concrete outside the critical section.

### **Load-Drift Relationships**

Relevant data collected during each specimen test are summarized in Table 2.

**Table 2-Specimen Test Data Summary**

Specimen	ND1C	ND2R	ND3R
1) Initial Gravity Load, $V_g$ (kN)	60.76	67.48	68.05
2) Initial Load/Shear Capacity Ratio	0.23	0.29	0.29
3) Gravity Load @ Failure (kN)	55.07	67.43	64.27
4) Maximum Horizontal Load (kN)	-30.87	-38.65	-41.72
5) Drift @ Maximum Horizontal Load (%)	-3	-3	-3
6) Maximum Drift Attained Before Failure (%)	8	4	5
7) Type of Failure	Flexure/Punch	Flexure*	Punch

\* Failure outside of the CFRP retrofit area.

These data include the initial gravity load supported by the column (row 1); the ratio between the initial gravity load and the shear capacity load at the critical perimeter (row 2); the gravity load at failure (row 3)—different from row 2 due to redistribution to the load rods; the maximum horizontal load during hysteresis (row 4); the drift level at the maximum horizontal load (row 5); the maximum drift level before failure (row 6); and the type of failure (row 7). The load-drift relationships for all specimens are shown in Figure 10. Figures 10a through 10c show the hysteretic response of specimens ND1C through ND3R respectively. Figure 10d is a comparison of the backbone curves—defined by the peak lateral load at each drift level—of the hysteretic response of these connections.

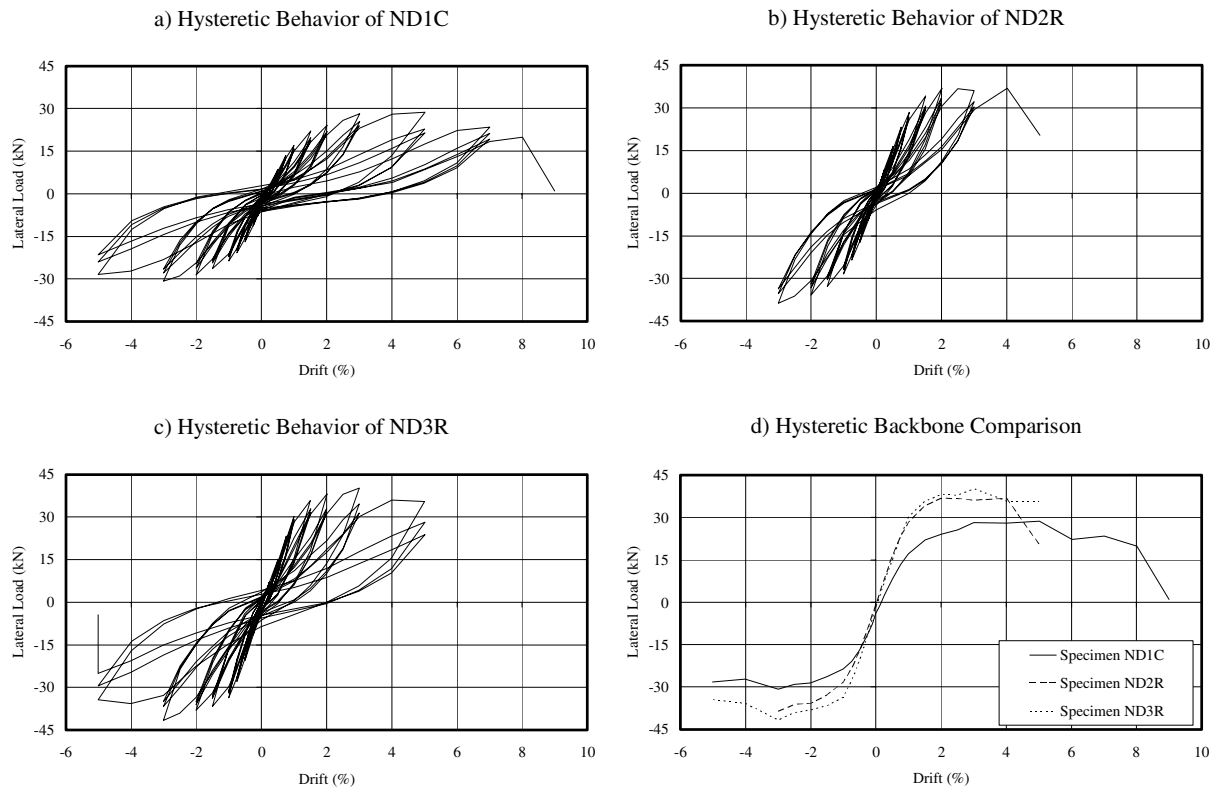


**Figure 10-Hysteretic Behavior of Specimens ND1C, ND2R, and ND3R.**

### Lateral Stiffness and Ductility

The following section describes the stiffness and ductility of the slab-column connections. The values of ductility are based on a derived yield point and hysteretic backbone curve of each connection as illustrated in Figure 11. Table 3 summarizes the derived ductility information of each specimen in both the positive and negative displacement directions. Extending a tangent to the initial stiffness (column 2) of the specimen to a point where it crosses the value of the peak lateral load (column 4) defines the yield point. The drift at this intersection is the yield drift (column 5). The peak ductility,  $\mu_p$ , (column 8) is the ratio

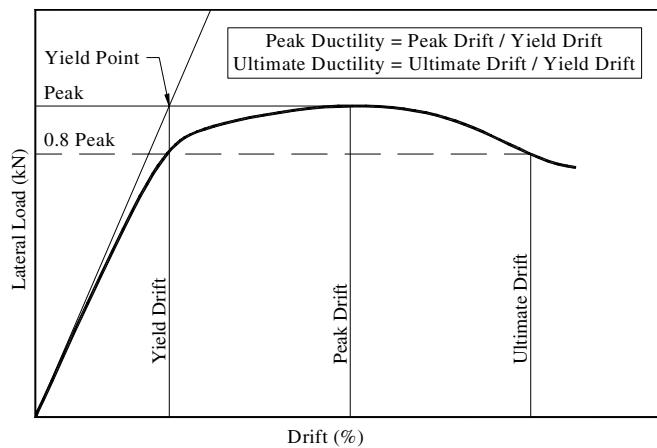


**Figure 11-Definition of Ductility Parameters.**

of the drift at the peak lateral load (column 6) to the derived yield drift (column 5). The ultimate ductility,  $\mu_u$ , (column 9) is the ratio between the ultimate drift (column 7) and the yield drift. The ultimate drift level is determined by three possible conditions; a punching shear failure, a reduction of the lateral load to 80% of the peak value, or the end of the cyclic routine (5% in the negative direction and 10% in the positive direction).

**Table 3-Retrofit Specimen Ductility Summary**

Specimen (+/- Drift Dir.)	Initial Stiffness (kN/%)	Gravity Shear at Peak Lateral Load, $V_u$ (kN)	Peak Lateral Load (kN)	Yield Drift (%)	Drift at Peak Lateral Load (%)	Ultimate Drift (%)	Peak Ductility ( $\mu_p$ )	Ultimate Ductility ( $\mu_u$ )
(1)	(2)	(3)	(4)	(5)	(6)	(7)	(8)=(6)/(5)	(9)=(7)/(5)
ND1C+	21.5	59.1	28.6	1.33	5	6 [9 <sup>†</sup> ]	3.76	4.51 [6.77 <sup>†</sup> ]
ND1C-	30.9	52.0	-30.9	-1	-3	-5*	3	5*
ND2R+	30.6	60.1	36.8	1.2	2	4	1.67	3.33
ND2R-	32.2	63.7	-38.7	-1.2	-3	-3	2.5	2.5
ND3R+	32.2	69.1	40.2	1.25	3	5	2.4	4
ND3R-	41.7	73.3	-41.7	-1.0	-3	-5*	3	5*

<sup>†</sup> Values when punching occurred. \* Ultimate drift limited by actuator stroke.

#### *Specimen ND1C*

The derived yield drift for specimen ND1C was between 1.0 and 1.33%. The initial stiffness was an average of 26.2 kN per percent drift. This specimen experienced a maximum horizontal load of 30.9 kN at a drift level of 3% as shown in Table 3. The specimen experienced a 20% loss of the peak lateral load (flexural failure) at a drift level of 6% and finally punched at a drift level of 9% (See the bracketed values in Table 2). The response to the loading shows a maximum peak ductility of 3.76 with an associated ultimate ductility of 4.51 [6.77<sup>†</sup>]. The horizontal load after punching decreased to 1.0 kN, 3% of the peak lateral load. The hysteretic response is shown in Figure 10a above.

#### *Specimen ND2R*

The derived yield drift for specimen ND2R was approximately 1.2%. The initial stiffness was an average of 31.4 kN per percent drift, a 20% increase over ND1C. This specimen experienced a maximum horizontal load of 38.7 kN at a drift level of 3% as shown in Table 3. This peak lateral load was a 27% increase in capacity over the control specimen. The horizontal load decreased to 35.9 kN before failure, 93% of the peak lateral load. The specimen failed in flexure at a drift level of 5%. The response to the loading shows a maximum peak ductility of 2.5 with an associated ultimate ductility of 2.5. The test was stopped for safety reasons due to the nature of the failure—flexural crack through the thickness of the unreinforced slab. The hysteretic response is shown in Figure 10b above.

#### *Specimen ND3R*

The derived yield drift for specimen ND3R was between 1.0 and 1.25%. The initial stiffness was an average of 37.0 kN per percent drift, a 41% increase over ND1C. This specimen experienced a maximum horizontal load of 41.7 kN at a drift level of 3% as shown in Table 3. This peak lateral load was a 38% increase in capacity over the control specimen. The specimen punched at a drift level of 5%. The response to the loading shows a maximum peak ductility of 3.0 with an associated ultimate ductility of 5.0. The horizontal load after punching decreased to 4.4 kN, 10% of the peak lateral load. The hysteretic response is shown in Figure 10c above.

Figure 12 shows a comparison of peak ductility. The results do not suggest any significant change in the peak ductility with the addition of the CFRP. This occurs because the yield drift and drift at peak lateral load are virtually the same in all three cases. Figure 13 indicates a decrease in ultimate ductility created by the addition of CFRP by comparing the ultimate drift levels observed during testing. Flexural failure of ND2R represented an ultimate ductility which was two-thirds of that for the flexural failure (80% decrease in lateral load capacity) of the control specimen (Figure 13a). Punching failure of ND3R represented an ultimate ductility approximately two-thirds of that for punching failure of the control specimen (Figure 13b). This criterion provides a more appropriate comparison since the flexural failure of ND1C at 6% drift does not represent a progressive collapse scenario but its punching failure at 9% does.

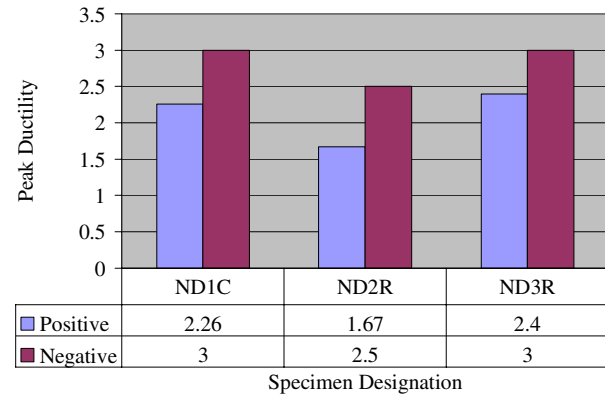


Figure 12-Comparison of Peak Ductility.

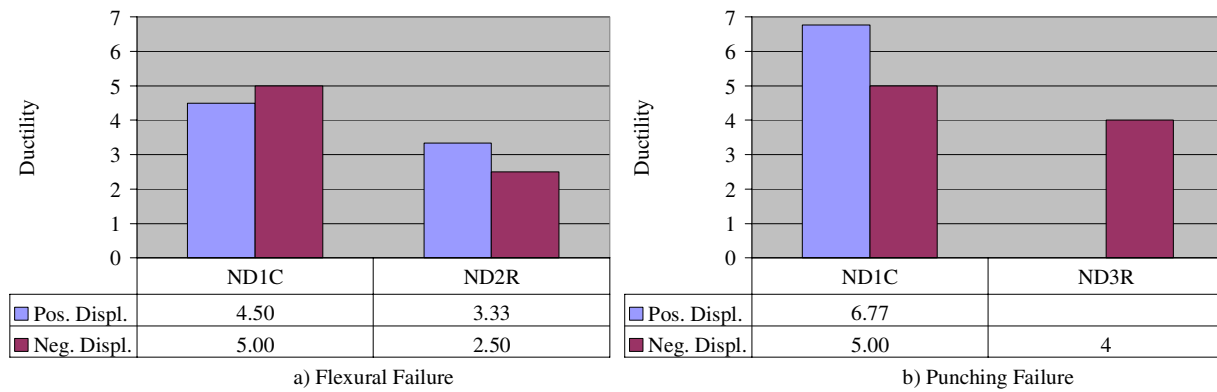


Figure 13-Comparison of Ultimate Ductility.

**Direct Punching Load-Deflection Results**

Specimens DPS1C and DPS2R were subjected to monotonic increasing direct punching shear. The load-displacement response of each specimen is shown in Figure 14. The addition of the CFRP shear studs only increased the punching capacity slightly. However, the ultimate deflection increased from 18mm to 44mm, an increase of 244%. This significant improvement in ductility suggests that these CFRP studs could be effective for seismic retrofit of slab-column connections. The authors are currently proceeding with cyclic lateral tests of slab-column connections retrofitted with CFRP headed studs.

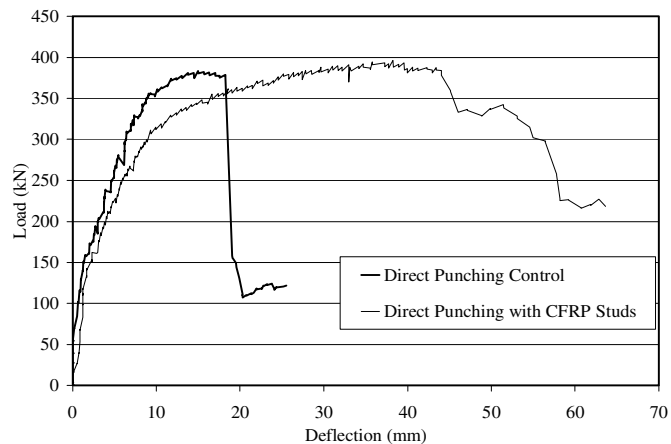


Figure 14-Direct Punching Load vs. Deflection.

## ANALYSIS

### Comparison with Current ACI Code Requirements

The ACI code provides a method to determine the combination of direct shear and unbalanced moment on a slab-column connection that will cause a punching failure. According to the code, the shear stresses are evaluated at a critical section around the column. This critical section is located at a distance of  $d/2$  from the face of the column, where  $d$  is the average depth of the tensile (top) steel from the compression surface (bottom) of the slab. The code method assumes that the shear at the critical section is the combination of the direct shear ( $V_u$ ) and a portion of the unbalanced moment ( $M_u$ ) at the connection.

Flexure and an eccentric shear stress on the critical section are assumed to transfer the unbalanced moment. The total maximum shear stress acting on the critical perimeter ( $v_u$ ) is determined from the following equation:

$$v_u = \frac{V_u}{A_c} \pm \frac{\gamma_v M_u c}{J_c}, \quad \text{Eqn. (1)}$$

where  $A_c$  is the area of the critical perimeter,  $J_c$  is the polar moment of inertia of the critical perimeter,  $\gamma_v$  is the proportion of the unbalanced moment transferred by eccentric shear stress, and  $c$  is the distance between the centroid and edge of the critical perimeter.

The concrete shear stress is limited to the smallest of three concrete stress equations given in ACI 318 Section 11.12.2.1. The slabs tested in this study are controlled by the following equation:

$$v_c = 1/3 \sqrt{f'_c}, \quad \text{Eqn. (2)}$$

where the concrete strength  $f'_c$  is in MPa.

### Lateral Specimens

The ACI code approach was applied to each of the slab-column specimens. Computed values and experimental results for the peak shear, unbalanced moment, and shear stresses around the critical perimeter for the retrofitted specimens were calculated and are presented in Table 4.

**Table 4-ACI 318 Comparison: Laterally Tested Specimen**

Spec.	Unbalanced Moment	Shear	Concrete Stress	Ultimate Shear Stress	Shear Ratio	Flexural Moment Capacity	Applied Moment	Moment Ratio
1	2	3	4	5	6	7	8	9
ND1C+	43.6	59.1	1.81	1.55	0.86	15.7	26.1	1.66
ND1C-	-47.0	52.0	1.81	1.59	0.88	15.7	-28.2	1.79
ND2R+	56.1	60.1	1.75	1.74	0.99	47.2	33.7	0.71
ND2R-	-58.9	63.7	1.75	1.97	1.13	47.2	-35.4	0.75
ND3R+	61.3	69.1	1.64	1.92	1.17	45.9	36.7	0.80
ND3R-	-63.6	73.3	1.64	2.16	1.32	45.9	-38.2	0.83

In Table 4 the first column contains the slab-column specimen designation. Each specimen has two rows; the first row refers to the peak lateral load in the positive direction, while the second row refers to the peak lateral load in the negative direction. The second column is the total unbalanced moment transferred from

the column to the slab at the peak lateral load. It is calculated by multiplying the peak lateral load by the story height of the specimen (1524 mm). Column (3) lists the total gravity load carried by the column at the peak lateral load. This value represents the total direct shear force acting on the slab at the critical perimeter.

The next three columns list the shear stress capacities of the slab at the critical perimeter. Column (4) is the concrete stress,  $v_c$ , calculated using equation 2. Since these slabs do not contain shear reinforcement, this represents the nominal shear stress capacity of the slab-column connection at the critical perimeter,  $v_n$ . Column (5), is the maximum shear stress acting on the critical perimeter due to the direct shear force in column (3) and the portion of the unbalanced moment carried by eccentric shear,  $\gamma_v M_u$ . Column (6) is the ratio of the maximum shear stress induced by the loading condition at the peak lateral load to the nominal shear capacity of the connection. A value of 1.0 for the shear ratio in column (6) would indicate that the connection is on the verge of a punching shear failure according to the ACI Building Code.

Slab-column connections may also fail due to flexural failure. According to the ACI Code, the portion of the unbalanced moment not carried by shear is carried by flexure,  $\gamma_f M_u$ . These values are listed in column (7) of Table 4. If this moment exceeds the flexural moment capacity of a slab width of  $c_2 + 3h$  centered on the column,  $M_f$ , then the ACI Code predicts a flexural failure. Values of  $M_f$  are listed in column (8). The moment ratio, column (9), is the ratio of the unbalanced moment resisted by flexure to the nominal moment capacity of the slab within  $c_2 + 3h$ . A value in column (9) greater than unity indicates that the connection is carrying an unbalanced moment that is greater than that predicted by the ACI Building Code and flexural failure should result.

At the peak lateral load, the control specimen had an average shear ratio of 0.87 and an average moment ratio of 1.73. This indicates the observed flexural failure of ND1C with subsequent punching shear failure only after significant additional cycling to 9% drift.

The retrofitted specimens ND2R and ND3R had average shear ratios of 1.06 and 1.25 respectively and average moment ratios of 0.73 and 0.82 respectively. This would indicate that these specimens should fail due to punching shear prior to flexural failure at the face of the column. This was indeed the case for specimen ND3R, but specimen ND2R suffered premature flexural failure of the unreinforced slab away for the slab-column connection.

#### *Direct Punching Specimens*

When shear reinforcement in the form of stirrups or headed studs is used within the critical perimeter, the nominal concrete shear stress is reduced by half, i.e.  $v_c/2$ . The total shear capacity of the reinforcement is determined by the equations:

$$V_n = V_c + V_s, \quad \text{Eqn. (3)}$$

where

$$V_c = \frac{v_c b_o d}{2}, \quad \text{Eqn. (4)}$$

and

$$V_s = \frac{A_v f_y d}{s}, \quad \text{Eqn. (5)}$$

where  $A_v$  is the area of the shear reinforcement (i.e. cross-section of all legs on a perimeter around the column),  $f_y$  is the yield stress of the shear reinforcement, and  $s$  is the spacing of the shear reinforcement. To use this equation, the CFRP properties  $A_{fv}$  and  $f_{fu}$  were substituted in place of  $A_v$  and  $f_y$  in

conformance with ACI 440 [8]. The equivalent nominal shear stress due to the reinforcement at the critical perimeter then becomes;

$$v_s = \frac{V_s}{b_o d} \quad \text{Eqn. (6)}$$

The total nominal shear stress at the critical perimeter becomes the following:

$$v_n = v_c/2 + v_s \quad \text{Eqn. (7)}$$

with an upper limit of  $1/2 \sqrt{f'_c}$ .

Using the concrete and CFRP stud properties listed earlier, the total nominal shear stress for specimen DPS2R is 3.38 MPa compared with 2.58 MPa for specimen DPS1C without shear reinforcement. The punching shear capacity of DPS2R should therefore be 31% greater than DPS1C. The test results show only a slight increase in punching shear capacity, however the connection ductility increased significantly as discussed earlier.

## CONCLUSIONS

Two series of tests were performed on undamaged and retrofitted pre-1971 non-ductile slab-column connections. The first series were subjected to cyclic lateral loading. The second set of slab-column connections were subjected to direct punching shear.

Based on the results of cyclic tests performed on slab-column connections retrofitted with CFRP applied to the slab top surface, the following conclusions were drawn:

- The control specimen experienced a flexural failure followed by punching shear at 8% lateral drift.
- Retrofit using CFRP applied to the top of the slab increased both the lateral load capacity and the stiffness of the connection.
- The increased stiffness attracted more load to the connection and induced different failure mechanisms from that seen in the control specimen.
- In the retrofit specimen with CFRP on the slab around the slab-column connection, the lack of continuity in the slab top reinforcement resulted in premature flexural failure away from the column. This failure occurred at a lateral drift level of 4%.
- In the retrofit specimen with continuous CFRP on the top of the slab, this premature flexural failure was prevented, but the connection experienced a punching shear failure at 5% lateral drift.
- Both the ductility and lateral drift capacity were reduced by the addition of the CFRP retrofit.

Based on the results of the direct punching test of a slab-column connection retrofitted with CFRP headed studs, the following conclusions were drawn:

- The CFRP shear stud retrofit of the direct punching slab-column connection provided an increase in the punching displacement of 2.44 times that for the control non-retrofitted specimen.
- The CFRP shear stud retrofit in the configuration tested did not increase the direct punching capacity of the connection by the amount anticipated by ACI 318/440.
- Application of the CFRP shear studs for seismic retrofit of slab-column connections holds promise.

## ACKNOWLEDGEMENTS

The authors wish to thank Adriano “A.B.” Bortolin of Sika Products USA for donation of all carbon fiber and epoxy materials used in this study. The authors also thank Chandler Rowe and his colleagues at Plas-Tech Ltd., Hawaii, for donation of their time, labor and expertise in performing the retrofit on the cyclic test specimens.

## REFERENCES

1. FEMA. “FEMA-274 Commentary on the Seismic Rehabilitation of Reinforced Concrete Structures.” Federal Emergency Management Agency, Washington D.C. 1997: pp. 6-1 – 8.
2. Ghali, A. & Megally, S. “Stud Shear Reinforcement for Punching: North American and European Practices”, *Proceedings of the International Workshop on Punching Shear Capacity of RC Slabs*, Kungl Tekniska Hogskolan Institute for Byggekonstruktion, Stockholm, Sweden. 2000: pp. 201-209.
3. Dovich, L. & Wight, J. K. “Lateral Response of Older Flat Slab Frames and the Economic Effect on Retrofit”, *Earthquake Spectra* 1996; 12(4): pp. 667-691.
4. Farhey, D. N., Adin, M. A., & Yankelevsky, D. Z. “Repaired RC Flat-Slab-Column Subassemblages under Lateral Loading”, *Journal of Structural Engineering*, November 1995: pp. 1710-1720.
5. Johnson, G. & Robertson, I. N. “Seismic Repair and Retrofit of Reinforced Concrete Slab-Column Connections using CFRP.” University of Hawaii Report UHM/CE/01-04, May 2001: pp. 134.
6. ACI Committee 318. “Building Code Requirements for Reinforced Concrete (ACI 318-99)” American Concrete Institute, Detroit, 1999.
7. ICRI. “Selecting and Specifying Concrete Surface Preparation for Sealers, Coatings, and Polymer Overlays: Guideline 03732”. Intl. Concrete Repair Institute, Sterling Virginia, 1997: pp.43.
8. ACI Committee 440. “ACI 440R-02 – Guide for the Design and Construction of Externally Bonded FRP Systems for Strengthening Concrete Structures”. American Concrete Institute, Detroit, 2002.